Received: 3 September 2020 | Revised: 8 December 2020 | Accepted: 18 January 2021

IET Power Electronics

DOI: 10.1049/pel2.12083

The Institution of Engineering and Technology WILEY

ORIGINAL RESEARCH PAPER

Failure analysis and lifetime assessment of IGBT power modules at low temperature stress cycles

Magnar Hernes[1] | **Salvatore D'Arco**[1] | **Antonios Antonopoulos**[2] | **Dimosthenis Peftitsis**[3]

[1] SINTEF Energi AS, Trondheim, Norway

[2] School of Electrical and Computer Engineering, National Technical University of Athens, Iroon Polytechniou 9, Zografou, Greece

[3] Department of Electric Power Engineering, Norwegian University of Science and Technology NTNU, O.S. Bragstadsplass 2E, Trondheim, Norway

Correspondence
Dimosthenis Peftitsis, Department of Electric Power Engineering, NTNU, O.S. Bragstadsplass 2E, 7491, Trondheim, Norway.
Email: dimosthenis.peftitsis@ntnu.no

Funding:
Research Council of Norway (Norges Forskningsråd), Grant number: 244010

Abstract

Lifetime models of high-power Insulated Gate Bipolar Transistors modules express the number of cycles to end of life as a function of stress parameters. These models are normally developed based on experimental data from accelerated power-cycling tests performed at predefined temperature stress conditions as, for example, with temperature swings above 60 °C. However, in real power converters applications, the power modules are usually stressed at temperature cycles not exceeding 40 °C. Thus, extrapolating the parameters of lifetime models developed using data from high-temperature stress cycles experiments might result in erroneous lifetime estimations. This paper presents experimental results from power cycling tests on high-power Insulated Gate Bipolar Transistors modules subjected to low temperature stress cycles of 30 and 40 °C. Therefore, devices experience still accelerated aging but with stress conditions much closer to the real application. Post-mortem failure analysis has been performed on the modules reaching end-of-life in order to identify the failure mechanism. Finally, the number of cycles to end-of-life obtained experimentally is fit with a state-of-the-art lifetime model to assess its validity at low temperature stress cycles. Challenges and limitations on data fitting to this lifetime model and the impact of various stress parameters on the anticipated failure are also presented.

1 | INTRODUCTION

Insulated gate bipolar transistors (IGBTs) are undoubtedly the most utilized power semiconductor switching devices in high-power converters due to their robust design and low conduction losses. However, power IGBTs are also vulnerable components and their failure leads to severe malfunctions or destructive failures of the power converters [1–4]. Thus, the understanding of the failure mechanisms for IGBT modules and the availability of verified lifetime models are critical for determining the reliability of power converters. Failure statistics from the field [5, 6] and accelerated power cycling tests (PCTs) [7, 8] have been utilized for assessing the reliability of IGBT power modules. However, the first method is rather impractical since it requires very long observation periods. Hence, the accelerated PCT is the approach generally adopted for assessing long-term reliability of high-power IGBT modules, as well as, for modelling their expected lifetime [3, 4].

Lifetime models for specific types of IGBT modules are developed by fitting experimental data from a large statistical population of devices under test (DUTs). These empirical lifetime models express the number of stress cycles to failure as a function of structural and operational parameters for the device such as: junction temperature swing, the minimum or the average junction temperatures, the heating and cooling times of the module, the heating current, as well as, IGBT and power module design parameters. Two notable empirical lifetime models, which are usually referred as LESIT [9] and CIPS08 [8] have been developed and documented in literature. Empirical lifetime models cannot distinguish between failure mechanisms and a post-mortem analysis is needed for confirming the dominant cause. Three distinct failure mechanisms have been identified on IGBT reaching end-of-life (EOL): bond-wire lift-offs, die-solder and substrate-solder delamination [3, 8, 10]. These mechanisms are developed simultaneously but the dominant cause of failure depends on the stress conditions.

During accelerated PCTs, the power module is stressed at a given temperature swing ΔT by periodically varying the junction temperature from a minimum to a maximum temperature while crucial IGBT parameters (e.g. collector-emitter voltage and junction temperature) are continuously monitored. It is a common practice to shorten the PCT duration by applying high stress conditions as a ΔT in the range of 40–80 °C [10–12]. The majority of IGBTs employed in power electronic converters operates with temperature stress cycles not exceeding $\Delta T = 40$ °C [13] and their lifetime is calculated by extrapolating the lifetime models developed with data acquired at high ΔT values to lower stress cycles values. However, this practice might trigger severe inaccuracies in the lifetime modelling and unrealistic estimation of results [14, 15], especially for ΔT lower than 30 °C where the module structure may be subjected to elastic deformation [16–18].

A first attempt to model IGBT power module lifetime at $\Delta T = 30$–80 °C has resulted in the development of the LESIT model [9]. The impact of health status preconditions of low-voltage IGBT power modules on assessing and accurately modelling their remaining lifetime at low ΔT values (i.e. $\Delta T = 28$–40 °C) has been investigated in [19, 20]. This revealed that the effect of low ΔT stress cycles becomes dominant in pre-aged modules with an accumulated degree of die-attach solder fatigue.

This paper presents an experimentally based investigation for high-power IGBT modules at low temperature stress cycles of $\Delta T = 30$ °C and $\Delta T = 40$ °C. Thus, the IGBT modules still experience accelerated aging and a failure within a practically reasonable timeframe but with stress conditions much closer to the real application. To the best knowledge of the authors, the CIPS08 model has not been experimentally validated for temperature cycles below 40 °C [2, 4, 10]. The paper contributes to providing experimental support to the validity of the CIPS08 lifetime model for IGBT power modules closer to real stress conditions for operation in converters. The effect of stress parameters on experimental data fitting, accuracy of the lifetime models and anticipated failure mechanism at low and high ΔT values is also investigated. In particular, the impact of the heating on-time period t_{on}, and heating current I on the failure modes, due to different inherent time constants of the module is assessed. Post-mortem analysis of the failed modules using visual inspection and Scanning Acoustic Microscopy (SAM) verifies the experimental findings.

The paper is organized as follows: Section 2 summarizes the fundamental PCT design and operating principle. Section 3 analyses the most relevant lifetime models for IGBT power modules and their associated limitations. The PCT experimental setup is described in Section 4 and the experimental results and post-mortem analysis are presented in Section 5. Fitting of the experimental data to the lifetime model for the IGBT power modules is shown in Section 6, including a discussion of the results. Conclusions are summarized in Section 7.

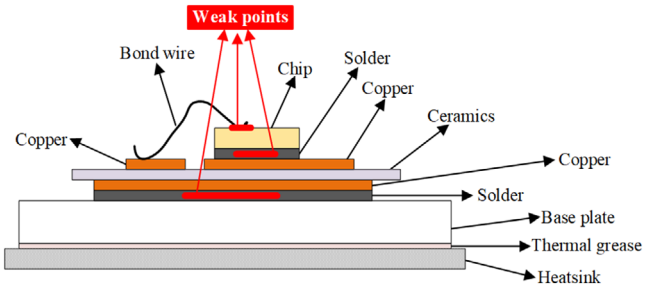

FIGURE 1 Typical internal layered structure of high-power IGBT modules indicating the spots for potential failures

2 | ACCELERATED POWER CYCLING TESTING METHODOLOGY

High-power IGBT dies are encapsulated in power module structures, which enable mechanical robustness for the dies and ease the electrical and mechanical connections with the converters bus-bar system and frame. An illustration of the typical structure of a power module is shown in Figure 1, where the internal layers, such as the copper layer for attaching the dies, the ceramic layer for insulation and the bond wires for electrical connections are depicted. These materials are characterized by different coefficients of thermal expansion. Thus, under extensive and long-term temperature stress, the temperature gradient in the junctions causes mismatches in the expansion of these inner layers, which eventually lead to development of stress forces between them, and consequently ageing. The specific stress condition dictates the anticipated failure mechanism. However, in practical applications it is also very likely that a combination of these failure mechanisms might occur. The weak points of the power module structure are highlighted with red colour in Figure 1.

The principle of the PCTs is to heat up the device under test until a maximum junction temperature T_{jmax} by forcing a current through the die for an on-time t_{on}. When T_{jmax} is reached, the heating current is turned-off and the DUT is cooled down until the initial temperature level T_{jmin} during the off-time period t_{off}. Active heating of the dies is achieved either by supplying dc power or by operating the power modules with ac power in a converter with a realistic mission profile [7]. The junction temperature could be either sensed directly or estimated by monitoring temperature sensitive electrical parameters (TSEPs) of the dies. However, due to the difficulty in accessing the dies in enclosed power modules structures, indirect measurement methods are preferred. For instance, sensing TSEPs, such as the collector-emitter on-state voltage of the IGBT or the forward voltage drop of the diodes is a commonly used methodology for junction temperature estimation [7].

Empirical lifetime models are developed based on PCT results and usually express the number of cycles to failure as a function of the ΔT stress, T_{jmin} or the average junction temperature, T_{javg}. In order to identify the number of cycles to

failure, end-of-life criteria are set. By monitoring the increase on collector-emitter voltage of the IGBT compared to the level at the start of the PCT, bond-wire fatigue can be detected [8]. On the other hand, solder delamination is detected by observing the rise in the thermal resistance of the power module [8, 21].

As the degradation of the monitored module parameters (e.g. solder and bond-wire fatigue) progresses during the PCT execution, variations of testing parameters might impact the test results. In particular, solder fatigue causes a higher junction temperature in the DUT, which results in an increasing ΔT during the PCT under constant current, t_{on}, t_{off} and cooling conditions. On the other hand, bond-wire degradation leads to an increased forward voltage of the DUT, and, thus, to an increasing ΔT under constant current. Therefore, controlling the testing parameters is very crucial for obtaining accurate results. Four control strategies for PCTs have been identified [22]: (1) constant t_{on} and t_{off}, (2) constant base plate temperature swing, (3) constant power dissipation in the DUT and (4) constant junction temperature swing.

It has been experimentally shown that the worst-case PCT methodology is achieved by keeping the on-time, t_{on}, and off-time, t_{off}, constant, since this strategy has no counter effect on any degradation [22]. Therefore, the adopted PCT methodology in this paper is based on constant t_{on} and t_{off} time periods.

3 | OVERVIEW OF POWER CYCLING LIFETIME MODELS FOR IGBT POWER MODULES

Empirical lifetime models are developed using a large amount of experimental PCT results obtained on different types of IGBT power modules and under various PCT testing conditions [23]. Typically, an empirical lifetime model expresses the expected lifetime span of a power module in terms of stress cycles to EOL. Apart from using experimental data acquired by accelerated PCTs, modelling and simulation of power modules using Finite Element Methods (FEM) software can speed up the extraction of useful results on lifetime estimation [24, 25]. Even in such cases, accurate modelling of power modules imposes the utilization of experimental data from PCTs, the measurement of TSEPs with the highest possible accuracy and the accurate modelling of the material characteristics [26]. Therefore, the scope of the presented experimental validation of the lifetime models for IGBT power modules is limited to the empirical models.

The two most notable lifetime models for IGBT power modules are the LESIT model, which is an evolution of the Coffin–Manson law [9], and the CIPS08 model [8]. This section presents an overview of these lifetime models, as well as, limitations and challenges associated with their applicability for estimating lifetimes of IGBT power modules operating under practical loading conditions.

3.1 | Coffin–Manson law and LESIT model

The first empirical lifetime model for modelling power cycling stress fatigue was introduced in the 70′s based on the Coffin–Manson law. According to this model, the number of cycles to failure, N_f, is assumed to decrease exponentially with the temperature swing of the junction temperature ΔT. The Coffin–Manson law, initially developed for estimating the fatigue in solid bodies [27], was expanded in the 1990′s to the, so-called, LESIT model [9]. In contrast to the Coffin–Manson law, the LESIT model takes into account the effect from the absolute junction temperature, T_j, by adding an Arrhenius factor to the initial expression as shown in Equation (1). In this equation R is the gas constant, $T_{j,avg}$ is the junction mean temperature, and Q is the activation energy. The empirical-based coefficients α and A are obtained by fitting experimental data.

$$N_f = A \cdot (\Delta T)^{a} \cdot e^{\left(\frac{Q}{R \cdot T_{j,avg}}\right)} \tag{1}$$

3.2 | CIPS08 model

The impact of a few additional testing parameters (i.e. the heating on-time, the minimum junction temperature, the current I per bond stitch) and power module design parameters (i.e. the breakdown voltage of the IGBTs V divided by 100 and the bond-wire diameter D) are taken into account in the CIPS08 model [8, 28]. By incorporating these additional parameters, the fitting of experimental data and accuracy of the lifetime model are significantly improved [8]. The CIPS08 lifetime model is expressed by Equation (2), which gives the cycles to failure, N_f, as a function of PCT conditions and power module design parameters.

$$N_f = k_b \cdot (\Delta T)^{\beta_1} \cdot e^{\frac{\beta_2}{T_{j,min}+273}} \cdot t_{on}^{\beta_3} \cdot I^{\beta_4} \cdot V^{\beta_5} \cdot D^{\beta_6} \tag{2}$$

In Equation (2), the β coefficients are extracted by properly fitting power cycling test results.

3.3 | Limitations and challenges on applying the lifetime models

PCT are generally conducted in accelerated conditions to reduce the duration of the testing within practically reasonable limits. The acceleration of the aging can be achieved mainly by increasing the amplitude of the temperature stress and/or by increasing its repetition rate. Increasing the stress amplitude leads to an exponential acceleration of the aging but extrapolating for lower temperature requires the assumption that the failure mechanism would not be significantly altered. The increase of the repetition rate leads to a linear acceleration and softer assumptions for extrapolating to normal user conditions because the failure mechanism is not substantially altered.

The original coefficients of the presented lifetime models have been extracted by fitting experimental data from accelerated PCTs that are usually performed at high ΔT values (e.g. >70 °C). However, in power converters operating with realistic mission profiles, the IGBT power modules are usually stressed at ΔT cycles lower than 40 °C. Thus, the applicability of the empirical lifetime models with their coefficients developed from PCT data acquired at high ΔT values might be critical for accurate lifetime predictions.

To the best knowledge of the authors, there is no experimental evidence justifying the application of lifetime models developed using high ΔT values to predict lifetime of IGBT power modules that are stressed at low ΔT cycles. The common practice is to extrapolate existing lifetime models developed at high ΔT values to lower temperature cycles [15] without sufficient experimental justification. However, it is highly likely that this methodology may give inaccurate results. For example, the application of the CIPS08 model without adapting to the actual type of module and temperature stress applied to the IGBTs in a high-power application could result in questionable lifetime estimations [14, 15, 16].

Another crucial limitation of the developed lifetime models is related to the PCT conditions. To reach a desired ΔT value, various combinations of PCT parameters, such as heating time, heating current and minimum or mean temperature of the dies can be imposed [8]. The choice of these PCT conditions has a large impact not only on the number of cycles to failure, but also on the type of failure [22]. These issues are partly investigated in this paper.

PCTs are performed at periodic stress cycles, which have a constant temperature swing. Thus, the applicability of these lifetime models and the fitting of their coefficients at combined stress cycles still remains an open challenge. Modelling of IGBT power modules lifetime under varying ΔT conditions has been reported in [29, 30]. In these works, the total lifetime due to the combined stress cycles has been estimated using the rainflow-counting algorithm and the linear damage accumulation theory known as Miner's rule [31–34]. Validation of Miner's rule has been verified experimentally by studying the dependency of the on-time and the current per bond wire on the expected lifetime during an accelerated PCT [35]. Even though the lifetime consumption due to various stress cycles has been assessed using linear damage accumulation methods [31,32], the impact of low ΔT cycles on the anticipated failure mechanism and lifetime model validity still needs more investigations.

The main failure mechanisms from PCTs are die- and substrate-solder fatigue, and bond wire lift-offs. However, which mechanism dominates in each case of failure, strongly depends on the module design, and conditions the device has been subject to [36,37]. Empirical lifetime models such as (1) and (2) represent failures of all three types, but they are not able to indicate if a device has actually failed due to bond-wire lift-offs or solder fatigue. Several efforts are described in literature, aiming to study each of the failure mechanisms. The work presented in [38] focused on bond wire lift-off as the main failure mechanism, while more recent publications, as for example [9, 19] and [39] highlight the solder fatigue of the die as the dominant failure mechanism. It is assumed that the results obtained are to a high degree reflected by the variety of module technologies, as well as by the fact that there has been a significant technology development over the time span for all these publications. Moreover, the impact of each from the three failure mechanisms could depend on the stress condition, such as the heating on-time. Thus, the lifetime model adaption must be carefully made by taking into consideration the adjustment of the model coefficients, the operating conditions of the power modules, as well as the type of PCT experimental procedure and the data that the model are based on.

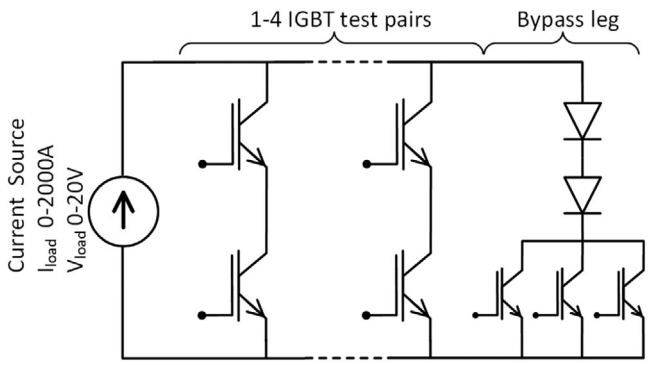

FIGURE 2 Schematic diagram of the PCT bench power circuit

4 | EXPERIMENTAL SETUP FOR ASSESSING IGBT LIFETIME

In order to assess the reliability of the DUTs and model their expected lifetimes at low ΔT values, experimental data have been acquired by performing a set of accelerated PCTs using high-power IGBT modules. These PCT experiments have been conducted using a PCT setup with the capability of simultaneously testing eight DUTs, as shown in Figure 2. The test circuit consists of four parallel legs, and each leg contains two series-connected IGBT modules along with all auxiliary and control circuits, as well as measurements sensors. A direct current source with the capacity of 2000 A supplies the required current to heat up the DUTs. Each testing slot is equipped with a custom-made water-cooled heatsink for guaranteeing sufficient and uniform cooling for all DUTs. Moreover, the cooling-water flow is finely regulated to ensure uniform cooling conditions for the DUTs. During the preparatory phase of the experimental setup and in order to ensure a realistic value for the thermal impedance between the IGBT junction and the ambient environment, manufacturer instructions regarding heatsink surface quality, application of thermal grease and mounting torques have been followed. Figure 3 shows a photo of the PCT experimental setup.

During the PCT, the four IGBT-pair legs sequentially conduct the direct load current based on a predefined switching pattern, where the on-period, t_{on}, for each of the four legs is

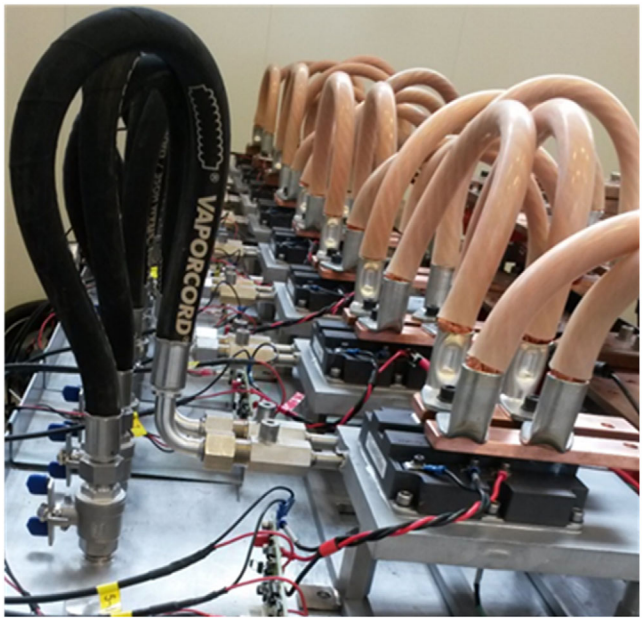

FIGURE 3 Photo of the power cycling test bench assembled with eight IHV 130 mm IGBT test objects

TABLE 1 Controllable and resultant testing parameters

Controllable test variables	Cooling water inlet to heat sink
	Coolant flow rate
	Load current
	Power on- and off-times (t_{on}/t_{off})
Aimed stress conditions	Minimum junction temperature ($T_{j\,min}$)
	Junction temperature swing ΔT

always equal to 25% of the total cycling period. In this way, the direct current supplied by the source flows continuously and the current source is not stressed by power cycling. After any of the DUTs fails, a bypass leg provides a continuous current path for the load current while the remaining operating DUTs continue with the same on-period and off-period patterns. Finally, the series-connected diodes with the bypass switch ensure that the voltage drops across the DUTs and the bypass leg remain constant during the experiments. The controllable variables for configuring the PCT are summarized in Table 1.

During the PCTs, several stress parameters are continuously monitored and logged, including the on-state collector-emitter voltage $V_{ce,load}$ of the IGBTs while the load current is flowing, and the case temperature T_c. The virtual junction temperature T_{vj} is estimated by applying a low-value sensing current through the DUT during the on-period of the IGBT while its load current is blocked by the adjacent IGBT. By measuring the resulting voltage $V_{ce,sense}$ as a TSEP, the virtual junction temperature can be estimated. In order to keep a linear relationship between $V_{ce,sense}$ and T_{vj}, the sensing current must be kept low (i.e., 500 mA for the present test objects). Measurements are acquired just before and after the turn-on instant, and just before and after the turn-off instant.

The thermal junction-to-case resistance $R_{th,(j\text{-}c)}$ is estimated using Equation (3) and based on the temperature measurements at the time instants just after the turn-on (cold state) and just before the turn-off (warm state) of the DUTs.

$$R_{th,(j-c)} = \frac{T_{vj} - T_c}{V_{ce,load} \cdot I_{load}} \tag{3}$$

An increase of $R_{th,(j\text{-}c)}$ is used as an indication of solder layers degradation while an increase of $V_{ce,load}$ indicates degradation of bond wires. A 20% increase of $R_{th(j\text{-}c)}$ or a 5% increase of $V_{ce,load}$ with respect to their initial values are assumed as the EOL criteria [8].

5 | EXPERIMENTAL RESULTS

5.1 | Overview of the test cases

A set of experimental PCTs has been conducted for validating the CIPS08 lifetime model at relatively low stress levels which represent more realistic stress conditions for IGBT modules in power converters than the conventional accelerated tests. The main challenge with the lower stress levels is the significantly increased duration of the PCTs until the DUTs fulfil an EOL criterion. While the normal operating range for a converter might be as low as a few tens of degrees, running PCTs at ΔT of 20 °C can lead to test periods longer than a year. Therefore, as a compromise, test runs were performed at ΔTs of 30 and 40 °C, since these stress levels are significantly lower than in accelerated conditions, but still allow completing the tests within a reasonable timeframe. An additional test case with accelerated conditions at a ΔT of 70 °C was added for model calibration. The hypothesis is that if the lifetime model parameters are valid for accelerated stress conditions, and they also fit well with lower-stress conditions, this could increase confidence of the model representativeness at these lower-stress conditions. Another important potential conclusion could be that the test objects were subject to plastic deformation at lower-stress conditions.

The DUTs were selected from the latest generation IGBT power modules with high voltage and high-power ratings (i.e. 3300 V/1000 A IHV-type IGBT modules). Such IGBT power modules are the most likely power-semiconductor candidates for medium- and high-voltage power converters utilized in a wide range of industrial and utility applications. Five PCT runs have been performed, each comprising eight IGBT DUTs tested simultaneously. The aim is to consider different stress parameters and achieve a sufficient statistical-population coverage of DUTs and stressing conditions. Given that the present materials and manufacturing technologies for power modules are mature, only small differences among the DUTs are expected, so the aforementioned number of samples is considered sufficient for statistical support. Thus, only small variances are anticipated in the PCT results for DUTs stressed under the

TABLE 2 Testing parameters for the five sets of test runs

		Test run number #				
		1	2	3	4	5
Controllable variables for the five test runs	Load current, I_{load} [A]	1250	1250	1250	890	890
	On-time, t_{on} [ms]	750	250	150	4500	1100
	Off-time, t_{off} [ms]	3250	750	450	13500	3300
	Coolant flow rate [l/min]	80	80	80	80	80
Resulting stress conditions	Junction temperature swing, ΔT [°C]	70	40	30	70	40
	Minimum junction temperature, $T_{j,\min}$ [°C]	60	60	60	60	60

same testing conditions, which was also confirmed during the PCTs.

Since this experimental validation involves only one type of IGBT power module, the structure-related parameters can be omitted in this investigation. Therefore, the number of variables in the CIPS08 lifetime model of (2) can be reduced by merging the blocking voltage term, V, and the bond-wire diameter, D, into one constant K, such as:

$$N_f = K \cdot (\Delta T)^{\beta_1} \cdot e^{\frac{\beta_2}{T_{j,min}+273}} \cdot t_{on}^{\beta_3} \cdot I^{\beta_4} \quad (4)$$

where $K = K_{fe} \cdot V^{\beta 5} \cdot D^{\beta 6}$.

During the tests, the minimum junction temperature $T_{j,min}$ was also kept constant at 60 °C for all PCT runs. Thus, the model in Equation (4) can be further reduced by incorporating the Arrhenius term into the constant K_2

$$N_f = K_2 \, \Delta(\Delta T)^{\beta_1} \Delta t_{on}^{\beta_3} \Delta I^{\beta_4}. \quad (5)$$

The main focus of the experimental testing is on the temperature stress ΔT, which is expected to have the strongest impact on the power-cycling lifetime. However, in order to impose a predefined ΔT, both the applied current I and the heating on-period t_{on} must be properly coordinated. It should be noted that several combinations of values for I and t_{on} will result in the same ΔT but with different heating profiles. This could affect the failure mode triggered in each case, being either bond wire or solder degradation.

The operating and testing parameters of the five PCT runs are summarized in Table 2. In the three first test runs, the selected ΔT values are obtained by adjusting the IGBT on-period t_{on} while maintaining a fixed test current that is equal to 1.25× the rated current (i.e. 1250 A). This choice of testing parameters results in a temperature slew rate of approximately 80 °C/s. For the 4th and 5th test run the current was set to approximately 0.9× the rated current (i.e. 890 A) leading to a lower temperature slew rate and requiring significantly longer on-periods to achieve comparable ΔTs to the first three test runs. A qualitative illustration of the two heating profiles for the five test cases is given in Figure 4. From this figure, a steeper temperature increase is associated with the first three tests and a slower gradient is used in the last two testing cases.

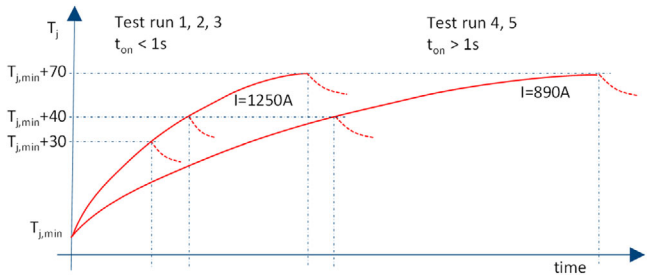

FIGURE 4 Qualitative illustration of the heating temperature profiles for the five tests runs

TABLE 3 Results of the electrical characterization of the DUTs

Test no.	No. of DUTs affected	Measured anomalies in post characterization measurements
1	2 of 8	Gate leakage
2	6 of 8	Gate leakage and/or blocking voltage failure
3	2 of 6*	Gate leakage
4	1 of 8	Gate leakage
5	0 of 6 *	None of the DUTs has been affected

*Two DUTs were taken out of the PCTs before reaching EOL, and they were used as DUTs for another test program.

5.2 | Failure analysis

In order to support the evaluation and conclusions of the experimental PCT results, pre- and post-electrical characterizations have been performed to all DUTs. The electrical characterization of the DUTs included an assessment of collector-emitter forward characteristics, gate-leakage current, gate-threshold voltage, and voltage-blocking characteristics. Furthermore, a selection of DUTs was subject to dissection for performing an internal visual and mechanical inspection of bond wires and emitter metallization.

A summary of the electrical pre- and post-characterization results is presented in Table 3. It is shown that the most affected device parameter is the gate leakage current and that no degradation was observed for the forward voltage and the gate-threshold voltage of the IGBTs. Long-term stress of the IGBTs under high-temperature conditions can result in degradation of

TABLE 4 Summary of the EOL detection indicators

Test no.	EOL indicator	No. of DUTs	The average of status for the other indicator	
			$R_{th(j\text{-}c)}$	$V_{ce\ load}$
1	$V_{ce,load} > 5\%$	8 of 8	~4%	
2	$V_{ce,load} > 5\%$	8 of 8	~3%	
3	$V_{ce,load} > 5\%$	6 of 6	~3%	
4	$V_{ce,load} > 5\%$	3 of 8	~16%	
	$R_{th(j\text{-}c)} > 20\%$	5 of 8		~4%
5	$V_{ce,load} > 5\%$	6 of 6	~7%	

the gate-oxide [17, 40] that is indicated by the increased gate leakage current. As an example, the gate leakage current for one of the DUTs used in the 4th test run was measured to be 25 mA at a gate-emitter voltage of $V_{ge} = 1$ V, which clearly indicates failure of the gate oxide. Furthermore, a few DUTs lost their blocking-voltage capabilities.

Table 4 summarizes the specific EOL indicators for the five runs of PCT experiments. This table clearly indicates that the failure indicator for all DUTs during the 1st, 2nd, 3rd and 5th PCT runs is a 5% increase of $V_{ce,load}$. The exception is the 4th test run, where the majority of the DUTs reached EOL by 20% increase of $R_{th(j\text{-}c)}$.

It should be mentioned that the PCT monitoring system is capable of measuring $V_{ce,load}$ at both the cold state (just after turn-on), and the warm state (just before turn-off). The on-state voltage is the sum of the chip voltage and the voltage drop of the module wiring, including the bond wires. For the 5% detection level of $V_{ce,load}$, the initial voltage condition was used as reference. However, increasing values of $T_{j,max}$ were observed during the ageing process for some PCTs, which introduced an increasing temperature offset for the voltage across the chips. Thus, the estimated voltage needs to be compensated for in the warm state $V_{ce,load}$ monitoring of the bond wire condition. For all tests only small variations were observed for $T_{j,min}$, and therefore, the cold-state chip voltage was assumed to be stable during the ageing process. The EOL criterion for $V_{ce,load}$ shown in Table 4 is the result from detecting a 5% increase of both the compensated warm-state temperature, as well as the uncompensated cold-state progress of $V_{ce,load}$. Any of these two voltages exceeding the 5% criterion first would trigger an EOL condition for the DUT.

A selection of DUTs was subjected to visual and mechanical inspection of the bond-wire condition and to microscopy investigation of emitter metallization. Figure 5 shows a picture of one DUT from the 2nd test run, where detached bond wires of one IGBT chip are clearly visible. Furthermore, several bond wires with seemingly good connection were easily detached by applying weak mechanical forces. Indeed, none of the inspected DUTs from the five test runs could be declared as 100% healthy in terms of bonding quality after test.

Clear indications of reconstruction of chip metallization were also found on several DUTs, as illustrated in Figure 6 for one of

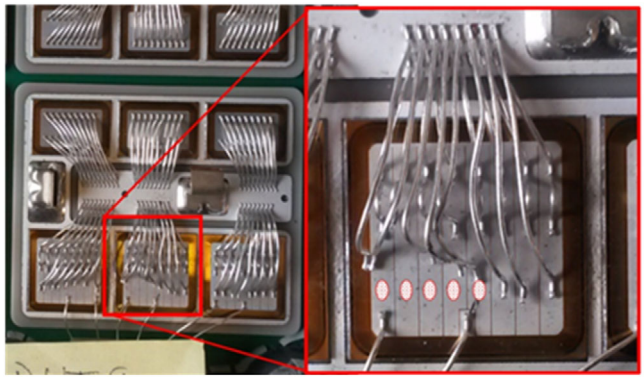

FIGURE 5 Photo of the post-analysis of a DUT from the 2nd PCT run showing detached emitter bond wires. Red pads illustrate the locations where bond wires are detached

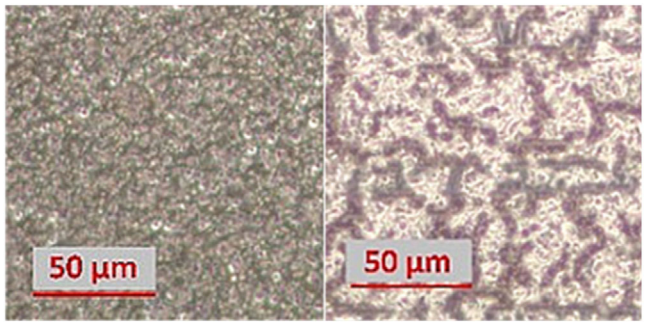

FIGURE 6 Microscopy images of emitter metallization. To the left, unused surface. To the right, post-mortem investigated DUT from the 1st PCT run

the DUTs. The reconstruction of the aluminium emitter metallization is primarily related to the bond wire fatigue [41] and causes increasing surface resistance in the aluminium layer. Figure 6 illustrates the status of chip metallization of a DUT used for the 1st test run, where all DUTs failed due to bond wire lift-offs (Table 4).

Pre- and post-mortem SAM analysis was also performed to several DUT samples from all five PCT runs for inspection of possible change or deterioration of the chip or the system solder layers. The main conclusion is that all DUTs were deemed healthy, apart from a few DUTs from the 4th test run, where a delamination growth tendency within the system solder layer was observed, as displayed in Figure 7. These observations

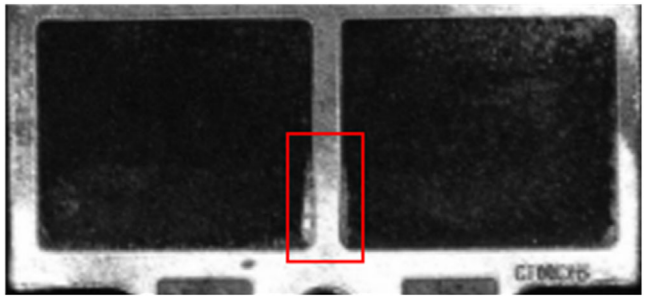

FIGURE 7 Recorded N_f versus ΔT for the five test runs

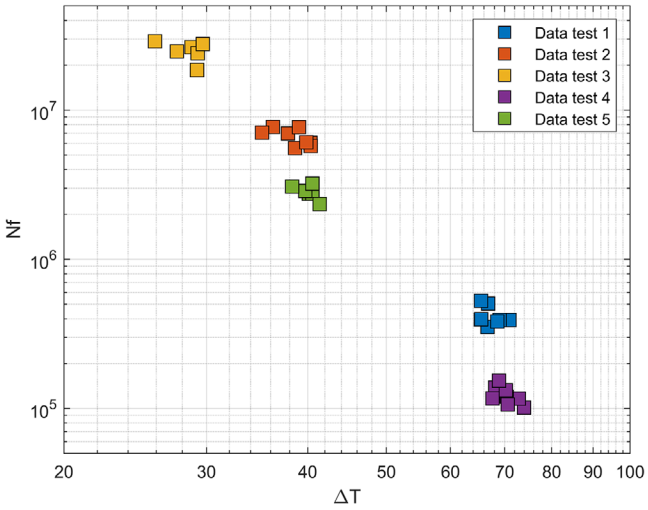

FIGURE 8 Inceptive delamination of system solder (red rectangle) for one DUT of the 4th test run

TABLE 5 Recorded span of ΔT and N_f for the 5 sets of test runs

Test no.	ΔT min/max [°C]	N_f min/max[cycles]	Net test duration [days]
1	65.4 – 70.9	351.900 – 528.051	18
2	35.1 – 40.3	5.562.900 – 7.723.300	90
3	25.9 – 29.7	18.602.000 – 28.932.000	201
4	68.2 - 74	101.290 – 153.490	32
5	38.3 – 41.4	2.341.900 – 3.218.636	164

confirmed the findings shown in Table 4, regarding the status of $R_{th(j\text{-}c)}$ after EOL.

The resulting lifetime for all DUTs and all sets of test runs is shown in Figure 8. Table 5 summarizes the resulting span of ΔT and the number of power cycles to EOL, N_f, for the five test runs, as well as the net duration for the PCTs.

5.3 | Discussion of the test results

As shown in Table 4, the observed EOL criterion for the majority of DUTs was a 5% increase in $V_{ce,load}$, which indicates bond-wire fatigue. However, a different situation was revealed in the 4th PCT run (low I, long t_{on}, high ΔTs), where five out of eight DUTs reached their EOL by fulfilling the R_{th} increase-detection criterion. The $V_{ce,load}$ for these five DUTs was also close to its EOL indication level, as shown in Table 4. During the same test run, the remaining three DUTs demonstrated a 5% increase of $V_{ce,load}$ before reaching the R_{th} detection level of 20% (which was also approached). It should be noticed that for the 4th test run, the on-period is relatively long compared to the other PCT runs. Furthermore, for the 4th test run, signs of development of solder fatigue were observed by SAM analysis. Based on these observations, it can be concluded that for PCT runs with the on-period up to the range of 1 s, the main ageing mechanism of the DUTs is bond-wire lift-offs. The longer on-periods for the 4th test run seem to trigger solder fatigue, and in this case probably both failure mechanisms are present.

Considering that the 1st and the 4th test runs are representing accelerated test conditions with ΔTs in the range of 70 °C, there is an interesting observation to be made: the resulting (average) N_f for the 4th test run is lower compared to the 1st one, even though the test current was lower for the 4th PCT. This is an indication that, judging only by the temperature swings ΔT and the stress current I, may lead to contradicting results. This fact supports that the on-period, and potentially more stress variables must be taken into account for a proper lifetime modelling.

The electrical post-characterization presented in Table 3 did not reveal any significant degradation of the bond-wire conditions by the forward voltage-drop measurement. Indeed, for most of the DUTs, the measured $V_{ce,load}$ at rated current was significantly lower than the 5% EOL detection level. A possible explanation is that, while inspecting the bond wires, even though they were detached from the emitter metallization, quite a few of them were still loosely maintaining their contact position assisted by the surrounding silicone gel. During the short current pulse (i.e. 300 μs) applied for the post-characterization of the forward voltage-drop, the contact position was probably well maintained, while during the significant longer t_{on} pulses by the PCT, the bond wires were subject to significantly more heating, followed by the increased contact resistance. Since the internal inspection revealed really poor conditions for the bond wires, it is also questionable whether the electrical offline characterization is adequate or the 5% detection level for the online $V_{ce,load}$ is too high. In order to determine the real condition for the EOL of the test objects, an internal inspection is essential.

6 | FITTING EXPERIMENTAL RESULTS INTO LIFETIME MODELS

As indicated previously, the CIPS08 model is selected for the assessment of the experimental data, due to the higher number of stress variables considered there. The applied PCT strategy with constant on-period (instead of varying t_{on} to keep ΔT constant) results in significantly higher stress conditions during the test run, mainly through increasing ΔT [22]. Indeed, when considering the average values of ΔT for the complete test runs, these values were in average ~4% higher compared to the initial values. Therefore, the assessment was made using data from both the initial (ideal) stress conditions, as well as the average values for the complete test runs. The following fitting process is based on the average values.

The model coefficients have been identified by least-square fitting of the test results using the numerical processing software MATHCAD. The fitting process is explained in detail in the following subsections. The accuracy of the fitting was assessed by comparing the deviation between the average of the recorded lifetimes for the samples during each PCT run, $mean(N^i_{f,n})$, and the prediction of the model for the same test-run conditions,

TABLE 6 Results of fitted coefficients from modelling approaches

Modelling effort name	Fitted coefficients	Fitted to test run #	Resulting coefficients: Fitted	Resulting coefficients: Original [8]
$M_{\beta\text{-CIPS08}}^{\#all}$	K	all	$K_e = 5.23\times10^{15}$	—
$M_{\beta\text{-}1}^{\#123}$	K, β_1	1, 2, 3	$\beta_{e1} = -4.73$	$\beta_1 = -4.42$
$M_{\beta\text{-}1}^{\#45}$	K, β_1	4, 5	$\beta_{e1} = -5.56$	
$M_{\beta\text{-}1}^{\#all}$	K, β_1	all	$\beta_{e1} = -5.34$	
$M_{\beta\text{-}14}^{\#all}$	β_1, β_4	all	$\beta_{e1} = -4.97$ $\boldsymbol{\beta_{e4} = +2.32}$	$\beta_1 = -4.42$ $\beta_4 = -0.72$
$M_{\beta\text{-}134}^{\#all}$	$\beta_1, \beta_3, \beta_4$	all	$\beta_{e1} = -2.07$ $\beta_{e3} = -1.42$ $\beta_{e4} = -4.1$	$\beta_1 = -4.42$ $\beta_3 = -0.46$ $\beta_4 = -0.72$
$M_{\beta\text{-}134}^{\#1245}$	$\beta_1, \beta_3, \beta_4$	1, 2, 3, 4	$\beta_{e1} = -2.24$ $\beta_{e3} = -1.35$ $\beta_{e4} = -3.76$	$\beta_1 = -4.42$ $\beta_3 = -0.46$ $\beta_4 = -0.72$

TABLE 6-A Results of fitted coefficients from modelling approaches

Modelling effort name	Fitted coefficients	Fitted to test run #	Resulting coefficients: Fitted	Resulting coefficients: Original [8]
$M_{\beta\text{-CIPS08}}^{\#all}$	K	All	$K_e = 5.23\times10^{15}$	—

$N_{fe,n}$, according to

$$\Delta_n = \frac{N_{fe,n} - \text{mean}\left(N_{f,n}^i\right)}{\text{mean}\left(N_{f,n}^i\right)} \ [\%] \tag{6}$$

The prediction $N_{fe,n}$ expresses the CIPS08 model estimation for the averaged stress conditions in the test run n, and $N_{f,n}^i$ is the number of experimental cycles for the i^{th} DUT sample during the same test run.

6.1 | CIPS08 model with original β-coefficients

As a first step, the test results were assessed against the CIPS08 model by assuming values for the model coefficients, as presented in [8]. Only coefficients β_1, β_3, and β_4 are relevant with these test runs, as the $T_{j,min}$ (reflected by β_2) was always regulated to 60 °C, and the structural characteristics of the DUTs (reflected by β_5, and β_6) are the same. Dependences on the structural parameters and the minimum junction temperature are embedded within the constant K, as discussed in Section 5.1. The value of K is estimated to ensure the best (least-square) fit for all test runs. The results of the fitting process are summarized in Tables 6-A and 7-A with this case referred as $M_{\beta\text{-CIPS08}}^{\#all}$, and the test results along with the model-estimated values are shown in Figure 9.

TABLE 7 Deviations between estimated and resulting EOL for modelling approaches

Modelling effort name	Deviation Δ_n [%] between estimated and resulting EOL, according to (6): Run 1	Run 2	Run 3	Run 4	Run 5
$M_{\beta\text{-CIPS08}}^{\#all}$	−26.50	−8.10	16.46	14.09	13.85
$M_{\beta\text{-}1}^{\#123}$	2.96	−7.49	1.86	183.29	76.03
$M_{\beta\text{-}1}^{\#45}$	−62.46	−46.38	−24.22	−0.42	−1.52
$M_{\beta\text{-}1}^{\#all}$	−39.95	−24.12	0.40	60.82	40.68
$M_{\beta\text{-}14}^{\#all}$	−7.09	−4.85	12.42	14.91	−18.56
$M_{\beta\text{-}134}^{\#all}$	0.70	−2.85	−0.91	−2.15	1.12
$M_{\beta\text{-}134}^{\#1245}$	0.11	−2.09	**1.2**	−1.8	0.604

TABLE 7-A Deviations between estimated and resulting EOL for modelling approaches

Modelling effort name	Deviation Δ_n [%] between estimated and resulting EOL, according to (6): Run 1	Run 2	Run 3	Run 4	Run 5
$M_{\beta\text{-CIPS08}}^{\#all}$	−26.50	−8.10	16.46	14.09	13.85

The results using the original β-coefficients from [8] indicate a rather poor fit for almost each test run, except for the test run 2 where the error is approximately 8% (deviations below 10% are marked by green colour). Even if the conditions during the test runs #1 and #4 were at quite high ΔTs (well within the spread of the samples used in [8]), the results seem to have significant deviations from the model estimation. This is an indication that the original coefficients in [8] may not be representative for these DUTs. The mismatch can be justified

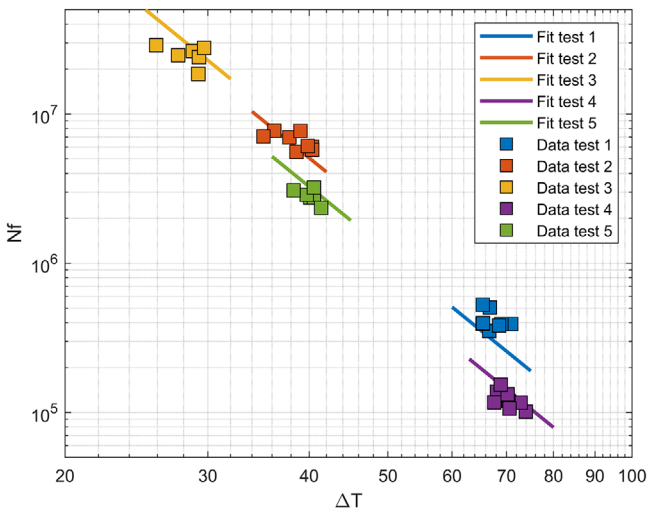

FIGURE 9 Recorded N_f versus ΔT for the five test runs and fitted graphs, when assuming the original CIPS08 β-coefficients

TABLE 6-B Results of fitted coefficients from modelling approaches

Modelling effort name	Fitted coefficients	Fitted to test run #	Resulting coefficients: Fitted	Resulting coefficients: Original [8]
$M_{\beta\text{-}1}^{\#all}$	K, β_1	all	$\beta_{e1} = -5.34$	$\beta_1 = -4.42$
$M_{\beta\text{-}1}^{\#123}$	K, β_1	1, 2, 3	$\beta_{e1} = -4.73$	
$M_{\beta\text{-}1}^{\#45}$	K, β_1	4, 5	$\beta_{e1} = -5.56$	

TABLE 7-B Deviations between estimated and resulting EOL for modelling approaches

Modelling effort name	Deviation Δ_n [%] between estimated and resulting EOL,according to (6)				
	Run 1	Run 2	Run 3	Run 4	Run 5
$M_{\beta\text{-}1}^{\#all}$	−39.95	−24.12	0.40	60.82	40.68
$M_{\beta\text{-}1}^{\#123}$	2.96	−7.49	1.86	183.29	76.03
$M_{\beta\text{-}1}^{\#45}$	−62.46	−46.38	−24.22	−0.42	−1.52

considering that the CIPS08 model coefficients have been derived from results on modules developed through different manufacturing processes. Additionally, there have been progressive technological improvements in IGBT power modules design during the last decade. Thus, to match the experimental results, a recalibration of the coefficients for the CIPS08 model is required.

6.2 | Fitting of the Coffin–Manson term

Temperature swings are associated to lifetime in the CIPS08 model by means of the Coffin–Manson term expressed by the coefficient β_1. Assuming that this term has the highest impact, a simple lifetime model can be formed as a first step, as in:

$$N_f = K_3 \cdot (\Delta T)^{\beta_1} \tag{7}$$

ignoring the impact of all other parameters. The coefficient value of the fitted β_{e1} is shown in Table 6-B, and the resulting deviation of this modelling effort to the results of each test run can be found in Table 7-B. Fitting the data points for all test runs (case $M_{\beta\text{-}1}^{\#all}$) leads to significant deviations for almost all data points. This indicates that the Coffin-Manson term alone is not sufficient for capturing the phenomena triggered by the stress, especially considering that differences in the temperature gradients could trigger different failure mechanisms.

One possibility to improve the results is to divide the test runs into groups, based on the applied current. Fitting the coefficients K and β_1 into the test results of each group (i.e., high-current group 1250 A, and low-current group 890 A), leads to the modelling efforts $M_{\beta\text{-}1}^{\#123}$ and $M_{\beta\text{-}1}^{\#45}$ respectively, also shown in Tables 6-B and 7-B. Each group of test runs presents particularly good fit this time with its corresponding lifetime estimation; however, the coefficients calculated in both cases fail to represent the data sets that correspond to a different current level. This further supports the claim that the Coffin-Manson lifetime model cannot sufficiently capture different stress conditions. However, it could provide a good insight even at low temperatures, provided that other stress factors (e.g. I and t_{on}) remain the same.

TABLE 6-C Results of fitted coefficients from modelling approaches

Modelling effort name	Fitted coefficients	Fitted to test run #	Resulting coefficients: Fitted	Resulting coefficients: Original [8]
$M_{\beta\text{-}14}^{\#all}$	β_1, β_4	all	$\beta_{e1} = -4.97$ $\boldsymbol{\beta_{e4} = +2.32}$	$\beta_1 = -4.42$ $\beta_4 = -0.72$

TABLE 7-C Deviations between estimated and resulting EOL for modelling approaches

Modelling effort name	Deviation Δ_n [%] between estimated and resulting EOL,according to (6)				
	Run 1	Run 2	Run 3	Run 4	Run 5
$M_{\beta\text{-}14}^{\#all}$	−7.09	−4.85	12.42	14.91	−18.56

6.3 | Extending the fitting to the other coefficients

The lifetime model in Equation (5) allows two additional degrees of freedom by fitting the coefficients β_3 and β_4. Having the indication from Section 6.2 that the current level makes a difference in the lifetime estimation, the next step is to add the current coefficient β_4 to the Coffin–Manson term. Results from all the test runs are considered as the modelling effort $M_{\beta\text{-}14}^{\#all}$. The fitted coefficients and the corresponding deviation are given in Tables 6-C and 7-C.

Comparing case $M_{\beta\text{-}14}^{\#all}$ with $M_{\beta\text{-}1}^{\#all}$, which both are processing all test runs, the introduction of the current term has significantly improved the overall results in terms of absolute deviation. However, the least-square fitting provides a positive value for β_4. A positive β_4 means that N_f is increasing with increasing load current, which is obviously wrong. This can also be observed directly by examining Figure 10.

The last step is to consider all three coefficients in Equation (5) in the fitting process (case $M_{\beta\text{-}134}^{\#all}$). As seen in Tables 6 and 7, where the results from all modelling efforts are included, the fitting results now present a fairly low deviation for all five test runs (below 3%), but the coefficients obtained are rather different from the original values given in [8]. The data sets from the test runs and the estimated lifetime for the respective test conditions according to the case $M_{\beta\text{-}134}^{\#all}$ fitting are shown in Figure 11.

It has been shown that, when using all three parameters in the modelling (ΔT, t_{on}, I), a fairly good fit can be obtained for all

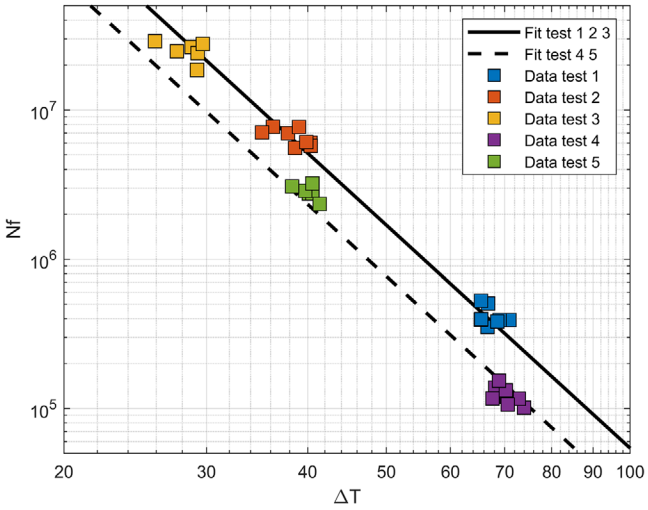

FIGURE 10 Recorded N_f versus ΔT for the five test runs and fitted graphs, representing subcase $M_{\beta\text{-}14}{}^{\#all}$

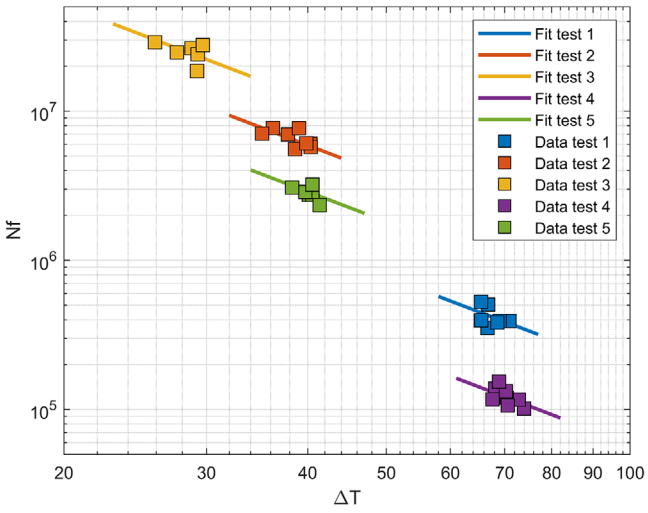

FIGURE 11 Recorded N_f versus ΔT for the five test runs and fitted graphs, representing subcase $M_{\beta\text{-}134}{}^{\#all}$

the test results. The question that remains open is if this model is sufficient to provide a good extrapolation to lower temperatures, which has been an important target of this investigation. To investigate that, a new modelling effort can be implemented, $M_{\beta\text{-}134}{}^{\#1245}$, considering all three coefficients in the fitting process, and all the test-run results, except for test run 3 (i.e. at a ΔT of 30 °C). If the coefficients calculated in this modelling effort can give a reasonable estimation that can be confirmed by the experimental results of the test run at 30 °C, this will provide a strong indication that this model can be extrapolated to 30 °C and maybe further below.

The coefficients resulting from the modelling effort $M_{\beta\text{-}134}{}^{\#1245}$ are shown in Table 6. It can be observed that the resulting values are similar to $M_{\beta\text{-}134}{}^{\#all}$. As expected, and shown in Table 7, this modelling effort provides good fit to the results of test runs 1, 2, 4, and 5. It is very important though, that the results from test run 3 are fitted very well too (only 1.2% deviation), without including these points in the process to calculate the coefficients.

6.4 | Discussion of the fitting results

It has been shown that by using the original stress coefficients of the CIPS08 model [8], the fit of the model to the PCT experimental results was rather poor. It has also been observed that the Coffin-Manson term can predict lifetime in the low-ΔT range if all stress parameters are kept stable.

When the fitting considers only the effect of the Coffin–Manson term and of the current term, the Coffin–Manson coefficient lies in the same range as the original value from [8]. However, the fitting was poor when results from all test runs were used in the fitting process. Even worse, for the same temperature swing, a positive value for β_4 was obtained. This implies that N_f increases by increasing load current, which is obviously wrong. This last observation clearly indicates that the power-on time needs to be included in the fitting process. The effect of the on-time is also considered in addition to the current and the Coffin–Manson in the last approach for the fitting. This resulted in a fairly good fit for all test runs. It is worth to notice that the resulting effect from the Coffin-Manson term and the on-time are in the same range. The sign of the current term is also reasonable. It is worth noticing that this last approach provides strong indications that the lifetime model can be extrapolated to stress level of 30 °C or even lower. However, at a lower ΔT the region of elastic deformation will be eventually reached, and the lifetime model will not be valid.

For the last approach, and with reference to Section 6, a separate fitting of model coefficients was done where the average values of the temperature swings for the complete test runs were replaced by the initial values. The resulting change of the β_1 coefficient was in the range of ∼0.5%, which is not regarded as crucial for the conclusions of this paper.

All results presented above are based on the measured virtual junction temperature, T_{vj}, since this is the common practice for accelerated PCT runs. The measurement of T_{vj} involves an unavoidable delay from the instant of IGBT turn-off until the time instant that the measurement is performed. This delay is approximately 1 ms for the experimental setup presented in Section 4. For the fitting of experimental results in this work, the possible impact from this delay was not considered. However, for the last approach, a separated fitting was done for investigating this effect. According to the measured thermal impedance characteristics Z_{th} for the DUT, the delay of 1 ms corresponds to a temperature drop of T_{vj} in the range of 2–3 °C, depending on the test current. By adjusting the temperature swings correspondingly, it was found that for the fitted model shown in Figure 11, the Coffin–Manson term, β_1 was changed from −2.07 to −2.2. Although not seen as crucial for the conclusion of the paper, this noticeable change will have an impact on the estimated lifetime. Therefore, such effects should be considered carefully before implementing power cycling lifetime models in real converter applications.

As a general trend, the fitted values indicate a significantly weaker effect of the Coffin–Manson term compared to the original coefficients. Moreover, it can be observed the significantly stronger impact of the terms associated to the current and on-time on lifetime. This may be seen as a further confirmation that different values for the on-time may induce different failure mechanisms. This also fits with the failure analysis presented in Section 5, where lower on-times were triggering failures in the bond wires, while the higher on-time of the test run 4 resulted in degradation of the solder layer.

It should be considered that due to the limited amount of test data and the measurement uncertainties, it is difficult to formulate a definitive statement regarding the fitted coefficients. Moreover, since only one test run indicated solder layer fatigue, the resulting coefficients should be assumed to represent primarily bond wire fatigue, while the validity for solder fatigue is significantly weaker.

The CIPS08 model [8] is using the minimum junction temperature as a parameter for the Arrhenius term. Therefore, all 5 accomplished test runs are assumed to have been subject to the same Arrhenius effect. However, the three different temperature swings were imposing different average temperatures. This raises a question whether a part of the Arrhenius effect in the CIPS08 is embedded in the Coffin–Manson term, implying that it might be interesting to investigate the effect of applying $T_{j,avg}$ instead of $T_{j,min}$ in this model.

7 | DISCUSSION AND CONCLUSION

This paper presented an experimental assessment of the CIPS08 lifetime model based on fitting experimental data from PCTs of high-power IGBT modules, also including low temperature stress cycles. By using the same type of DUTs for all the experimental work, and the same minimum junction temperature, it was possible to study the effect of junction temperature swings, current and power-on time on the expected lifetime. In addition to this, and by post-mortem analysis of the test objects, the impact of the specific PCT conditions on the anticipated failure mechanism has also been substantiated.

The analysis of PCT experimental results on power cycling of high-power IGBT modules at temperature cycles as low as 30 °C and their fitting to the CIPS08 lifetime model are the main contributions of this paper. In particular, the impact of various power cycling testing parameters on the anticipated failure mechanism has been assessed. It has been shown that temperature stress in the range of $\Delta T = 30$ °C and $\Delta T = 40$ °C still induces plastic deformations resulting in ageing of the IGBT power modules. However, it has been experimentally confirmed that the on-period has a strong impact and influences the failure mechanism. Indeed, low values of on-periods cause bond-wires lift-off, while longer values (i.e. longer than 1 s) trigger failures in the die-solder layer. It needs to be noticed that this assumption is based on the experimental results of the present test object and, therefore, cannot be regarded as a general conclusion. For example, in other works, [42] solder fatigue is concluded to be the dominant failure mechanism at low on-periods, while bond-wire fatigue at longer on-periods. It also needs to be noticed that other works, [43,44] do not confirm the findings of stronger impact from the current and on-period on the lifetime compared to the temperature stress swings. This is a reminder that the lifetime model, and especially the parameters, need to be fitted to the specific module technology.

The statistical data obtained from the PCTs have been processed to fit into the existing CIPS08 model and to determine its coefficients. Fitting experimental data from PCTs by only accounting the Coffin-Manson term results in a good fit for a given load current, but the model fails when considering experimental data with different currents. On the other hand, using the CIPS08 model, and by limiting the number of stress variables in the PCTs, it has been revealed that, the impact of the current and on-period on the lifetime is stronger compared to the weaker impact that the temperature stress swings impose. Especially the difference between the original and fitted CIPS08 coefficients resulted in a big deviation in the estimated power-cycling lifetime when the model is applied for a wide span of stress swings. Therefore, extrapolation of lifetime models to lower stress cycles must be performed with care and by not only considering the value of ΔT, but also and most importantly the utilized load current and operating profile in terms of temperature derivatives.

Through this work it has been verified that the CIPS08 model can be used to predict lifetime of IGBT power modules operating in practical power converters, which exhibit stress cycles of 30 °C and above. However, this requires a dedicated and time-consuming PCT experimental procedure for developing appropriate model coefficients for the specific type of IGBT modules employed in the converter. Special attention is required for model validation in the operating range where still plastic deformation is expected for the converter, i.e. stress cycles of 30 °C or even lower. Finally, it is emphasized that if the goal is to provide a lifetime model applicable for converters in operation, quite some additional power cycling experiments and model fitting need to be added to what has been presented in the present paper. For example, quite some more PCTs need to be performed at the lower range of stress cycles, and the model in Equation (5) used for fitting the coefficients also need to be extended by including the Arrhenius effect by the β_2 coefficient, Equation (4).

CONFLICT OF INTEREST

The authors declare no conflict of interest.

DATA AVAILABILITY STATEMENT

Author elects to not share data. Research data are not shared.

REFERENCES

1. Wang, B., et al.: Review of power semiconductor device reliability for power converters. CPSS Trans. Power Electron. Appl. 2(2), 101–117 (2017)
2. Song, Y., Wang, B.: Survey on reliability of power electronic systems. IEEE Trans. Power Electron. 28(1), 591–604 (2013)
3. Durand, C., et al.: Power cycling reliability of power module: A survey. IEEE Trans. Device Mater. Reliab. 16(1), 80–97 (2016)

4. Gopi, L.R., Reddy, L.M.T., Ozpineci, B.: Power cycle testing of power switches: A Literature survey. IEEE Trans. Power Electron. 30(5), 2465–2473 (2015)
5. Fischer, K., et al.: Field-experience based root-cause analysis of power-converter failure in wind turbines. IEEE Trans. Power Electron. 30(5), 2481–2492 (2015)
6. Vernica, I., Wang, H., Blaabjerg, F.: Design for reliability and robustness tool platform for power electronic systems-study case on motor drive applications. In: Proceedings of the IEEE Applied Power Electronics Conference and Exposition (APEC), San Antonio, TX, pp. 1799–1806 (2018)
7. Choi, U., Blaabjerg, F., Jørgensen, S.: Power cycling test methods for reliability assessment of power device modules in respect to temperature stress. IEEE Trans. Power Electron. 33(3), 2531–2551 (2018)
8. Bayerer, R., et al.: Model for Power Cycling lifetime of IGBT Modules - various factors influencing lifetime. In: 5th International Conference on Integrated Power Electronics Systems, Nuremberg, Germany, pp. 1–6 (2008)
9. Held, M., et al.: Fast power cycling test of IGBT modules in traction application. In: Proceedings of Second International Conference on Power Electronics and Drive Systems, Vol. 1, Singapore, pp. 425–430 (1997)
10. Choi, U., Jørgensen, S., Blaabjerg, F.: Advanced accelerated power cycling test for reliability investigation of power device modules. IEEE Trans. Power Electron. 31(12), 8371–8386 (2016)
11. Choi, U.M., Blaabjerg, F., Iannuzzo, F.: Advanced power cycler with intelligent monitoring strategy of IGBT module under test. Microelectron. Reliab. 76–77, 522–526 (2017)
12. Huang, Y., et al.: Lifting-off of Al bonding wires in IGBT modules under power cycling: Failure mechanism and lifetime model. IEEE J. Emerging Sel. Top. Power Electron. PP(99), 1–1 (2019)
13. Gierschner, S., Rump, T., Eckel, H.: Lifetime estimation for three level converter for wind energy application. In: 2015 IEEE 6th International Symposium on Power Electronics for Distributed Generation Systems (PEDG), Aachen, pp. 1–8 (2015)
14. Özkol, S.H.E.: Load-cycling capability of HiPak™ IGBT modules 5SYA2043-04. Tech. Report (2014)
15. Wang, L., et al.: Lifetime estimation of IGBT modules for MMC-HVDC application. Microelectron. Reliab. 82, 90–99 (2018)
16. Zhang, Y., et al.: Impact of lifetime model selections on the reliability prediction of IGBT modules in modular multilevel converters. In: 2017 IEEE Energy Conversion Congress and Exposition (ECCE), Cincinnati, OH, pp. 4202–4207 (2017)
17. Hartmann, S., Ozkol, E.: Bond wire life time model based on temperature dependent yield strength. In: The PCIM Europe 2012, Nuremberg (2012)
18. ABB, Load-cycling capability of HiPak IGBT modules, Application Note SYA 2043-04. (2014)
19. Lai, W., et al.: Low ΔTj stress cycle effect in IGBT power module die-attach lifetime modeling. IEEE Trans. Power Electron. 31(9), 6575–6585 (2016)
20. Lai, W., et al.: Experimental investigation on the effects of narrow junction temperature cycles on die-attach solder layer in an IGBT module. IEEE Trans. Power Electron. 32(2), 1431–1441 (2017)
21. Huang, Y., et al.: Failure mechanism of die-attach solder joints in IGBT modules under pulse high-current power cycling. IEEE J. Emerging Sel. Top. Power Electron. 7(1), 99–107 (2019)
22. Schuler, Scheuermann, U.: Impact of Test Control Strategy on Power Cycling Lifetime. In: The PCIM Europe 2010, Nuremberg (2010)
23. Busca, C., et al.: An overview of the reliability prediction related aspects of high power IGBTs in wind power applications. Microelectron. Reliab. 51(9–11), 1903–1907 (2011)
24. Li, H., et al.: Thermal coupling analysis in a multichip paralleled IGBT module for a DFIG wind turbine power converter. IEEE Trans. Energy Convers. 32(1), 80–90 (2017)
25. Kovačević, I.F., Drofenik, U., Kolar, J.W.: New physical model for lifetime estimation of power modules. In: The 2010 International Power Electronics Conference - ECCE ASIA, Sapporo, pp. 2106–2114 (2010)
26. Herold, C., et al.: Methods for virtual junction temperature measurement respecting internal semiconductor processes. In: IEEE 27th International Symposium on Power Semiconductor Devices & IC's (ISPSD), Hong Kong, pp. 325–328 (2015)
27. Lalanne, C.: Fatigue Damage, John Wiley & Sons, Hoboken, New Jersey (2014)
28. Lutz, J.: Packaging and reliability of power modules. In: CIPS 2014; 8th International Conference on Integrated Power Electronics Systems, Nuremberg, Germany, pp. 1–8.(2014)
29. Dbeiss, M., et al.: A method for accelerated ageing tests of photovoltaic inverters considering the application's mission profiles. In: 2017 19th European Conference on Power Electronics and Applications (EPE'17 ECCE Europe), Warsaw, (2017)
30. Huang, H., Mawby, P.A.: A lifetime estimation technique for voltage source inverters. IEEE Trans. Power Electron. 28(8), 4113–4119 (2013)
31. Choi, U., Ma, K., Blaabjerg, F.: Validation of lifetime prediction of IGBT modules based on linear damage accumulation by means of superimposed power cycling tests. IEEE Trans. Ind. Electron. 65(4), 3520–3529 (2018).
32. Zeng, G., et al.: Experimental investigation of linear cumulative damage theory with power cycling test. IEEE Trans. Power Electron. 34(5), 4722–4728 (2019)
33. Antonopoulos, A., et al.: Challenges and strategies for a real-time implementation of a rainflow-counting algorithm for fatigue assessment of power modules. In: *2019 IEEE Applied Power Electronics Conference and Exposition (APEC)*, Anaheim, CA, USA, pp. 2708–2713 (2019)
34. Yang, X., et al.: Lifetime prediction of IGBT modules in suspension choppers of medium/low-speed maglev train using an energy-based approach. IEEE Trans. Power Electron. 34(1), 738–747 (2019).
35. Jiang, N., et al.: Investigation of Ton dependency of Al-clad Cu bond wires under power cycling tests. In: *PCIM Europe 2018; International Exhibition and Conference for Power Electronics, Intelligent Motion, Renewable Energy and Energy Management*, Nuremberg, Germany, pp. 1–6 (2018)
36. Scheuermann, U., Junghaenel, M.: Limitation of power module lifetime derived from active power cycling tests. In: CIPS 2018; 10th International Conference on Integrated Power Electronics Systems, Stuttgart, Germany, pp. 1–10 (2018)
37. Schmidt, R., Scheuermann, U.: Separating failure modes in power cycling tests. In: 2012 7th International Conference on Integrated Power Electronics Systems (CIPS), Nuremberg, pp. 1–6 (2012)
38. Wuchen, W., et al.: Investigation on the long term reliability of power IGBT modules. In: *1995. ISPSD '95 Proceedings of the 7th International Symposium on Power Semiconductor Devices and ICs*. Yokohama, Japan, pp. 443–448.(1995)
39. Huang, H., Mawby, P.A.: A Lifetime Estimation Technique for Voltage Source Inverters. IEEE Trans. Power Electron. 28, 4113–4119 (2013)
40. Patil, N., et al.: Identification of failure precursor parameters for Insulated Gate Bipolar Transistors (IGBTs). In: International Conference on Prognostics and Health Management, Denver, Colorado, pp. 1–5 (2008)
41. Ciappa, M., Selected failure mechanisms of modern power modules. Microelectron. Reliab. 42(4), 653–667 (2002)
42. Junghaenel, M., Scheuermann, U., Impact of load pulse duration on power cycling lifetime of chip interconnection solder joints. Microelectron. Reliab. 76-77, 480–484 (2017)
43. Zeng, G., et al.: Power cycling results of high power IGBT modules close to 50 Hz heating process. In: 21st European Conference on Power Electronics and Applications (EPE '19 ECCE Europe), Genova, Italy, pp. 1–10 (2019)
44. Lutz, J., et al.: Validity of power cycling lifetime models for modules and extension to low temperature swings. In: 22nd European Conference on Power Electronics and Applications (EPE'20 ECCE Europe), Lyon, France, pp. P.1–P.9 (2020)

How to cite this article: Hernes M, D'Arco S, Antonopoulos A, Peftitsis D. Failure analysis and lifetime assessment of IGBT power modules at low temperature stress cycles. *IET Power Electronics*. 2021;1-13. https://doi.org/10.1049/pel2.12083